2020

Finite Element Modelling of the Interfacial Debonding Behaviour between Carbon Fibre Textile and Concrete

Stuka, K.

Stuka, K. (2020) 'Finite Element Modelling of the Interfacial Debonding Behaviour between Carbon Fibre Textile and Concrete', The Plymouth Student Scientist, 13(1), p. 328-348.
http://hdl.handle.net/10026.1/16515

The Plymouth Student Scientist
University of Plymouth

*The Plymouth Student Scientist, 2020, **13**, (1), 328-348*

Finite Element Modelling of the Interfacial Debonding Behaviour between Carbon Fibre Textile and Concrete

Kirstie Stuka

Project Advisor: Dr. Shanshan Cheng, School of Engineering, Computing and Mathematics (Faculty of Science and Engineering), University of Plymouth, Drake Circus, Plymouth, PL4 8AA

Abstract

This research deals with integrating finite element modelling into the investigation of the interfacial debonding behaviour between carbon fibre textile and concrete. A Cohesive Zone Model (CZM) replicating a pull-out simulation was initially validated and verified against a numerical model from an existing study, involving the single fibre pull-out from an epoxy matrix. The CZM was then modified by using experimental data obtained from a laboratory pull-out test involving a single carbon fibre tow embedded in a concrete matrix. By incorporating finite element modelling to the CZM, the modified numerical model was then able to successfully replicate the experimental force – displacement curve; producing a debonding force of 0.9082kN, closely matching up with the debonding force of 0.9021kN from the experiment.

The experimental debonding load was used as the basis for calibrating values for the maximum shear stress (τ_{max}) and complete separation displacement (δ_s). Through numerous trials and a series of adjustments, the carbon fibre tow – concrete matrix interface was found to have a maximum shear stress (τ_{max}) of 6.475MPa at a complete separation displacement (δ_s) of 0.775mm. The values corresponding to interfacial parameters defined in the study were only based on a single set of experimental results. This presents questionable issues regarding the validity and reliability of the findings. As a result, it is therefore recommended that multiple experiments be carried out in order to ensure that the calibrated $\boldsymbol{\tau_{max}}$ and $\boldsymbol{\delta_s}$ are both accurate and representative of the true interfacial behaviour.

Introduction

Carbon Fibre Background

Carbon fibres used in advanced composites contain a minimum of approximately 92% Carbon (Jia, Yan and Liu, 2011). Carbon fibres are known to have a low density; high stiffness; low thermal expansion and non-corrosive properties. Aside from this, these fibres consist of diameters no greater than 10μm and have tensile strengths that can range up to 6GPa. These properties have therefore generated significant interest in a variety of industries. Some of which include aerospace, civil, electronic and medical.

Carbon Fibre – Matrix Interface

Carbon fibres can be impregnated into a matrix such as epoxy or concrete in order to further enhance their desirable properties. The interface, occurring at the points of contact between the fibre and matrix influences the overall performance of the composite. Interfacial debonding occurs when composite action is no longer sustainable. This is a vital mechanism for the analysis of energy absorption. Numerous studies have been conducted in order to gain a better understanding of the influence that interfacial behaviour has on the mechanical behaviour of composites. From these studies also came the development of several techniques that could be used for the direct analysis of interfacial shear stress (Jia, Yan and Liu, 2011).

Single Fibre Pull-Out Test

The single fibre pull-out test is regarded as one of the most commonly used techniques for analysing interfacial shear strength. For this test to work effectively, the fibre length embedded into the matrix must be less than that of the critical embedded length for debonding. Not implementing this specified condition will result in the fibre rupturing prior to debonding. There are three key stages that take place during a single fibre pull-out test. These include elastic deformation (prior to debonding), interfacial debonding and sliding. During the deformation stage, the carbon fibre is bonded very well to the matrix. However, as the pull-out force gradually increases, an initial crack develops which then propagates along the entire fibre-matrix interface. This eventually leads to the complete debonding of the interface. During the final sliding stage, the fibre has completely debonded from the matrix and can now be pulled out. However, frictional forces acting between the newly formed surface of the fibre and that of the matrix affect the ease of fibre pull-out.

Cohesive Zone Modelling (CZM)

Cohesive Zone Modelling is another commonly used technique that focuses primarily on the energy-stress relationship through the analysis of interfacial behaviour. CZM places emphasis particularly on investigating fracture failure caused by crack propagation. The concept of CZM was originally proposed by Barenblatt (1959) and Dugdale (1960) and has been used extensively to stimulate composite fracture under static, dynamic and cyclic loading conditions.

The Cohesive Zone Law for mode II debonding is represented by the equation,

$$\boldsymbol{\tau_{is} = K\delta} \qquad \boldsymbol{0 \leq \delta \leq \delta_S}$$

Figure 1 illustrates the interfacial Cohesive Zone Law. The first portion of the curve defines the stiffness (*K)*, which equates to $\boldsymbol{K = \frac{\tau_{max}}{\delta_d}}$

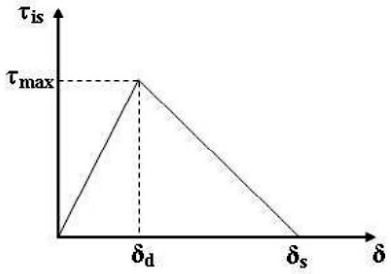

Figure 1: Interfacial Cohesive Zone Law
Reproduced with kind permission from Jia, Yan and Liu (2011)

A CZM establishes the relationship between traction – separation across an interface. The traction gradually increases until it reaches the peak bond strength, otherwise known as the maximum shear stress (τ_{max}). The initiate crack separation displacement (δ_d) corresponds to the τ_{max} and signifies the point at which the interface begins to fail by means of debonding. This failure is caused by the initial formation of a crack at the interface. From this point onwards, the crack progressively increases whilst the interfacial shear stress continually decreases. The complete separation displacement (δ_s) represents the point at which the interface has failed and completely debonded.

Numerous studies have investigated the interfacial behaviour between Fibre-Reinforced Polymer (FRP) and concrete under mode II conditions by means of experimentations, however very little has been done on using Cohesive Zone Modelling to numerically simulate a fibre pull-out test. The utilisation of CZM would be far more beneficial as it would provide a cost-effective alternative to lab experiments. Aside from this, obtaining results would be significantly faster.

Methodology

Finite Element Modelling of the Initial CZM

Prior to the development of the numerical model used for this research, one was initially created based on an existing study (Jia, Yan and Liu, 2011) which involved replicating the simulation of a single fibre pull-out test. Verification and validation of this initial CZM functioned to serve the basis for the numerical model of the current study.

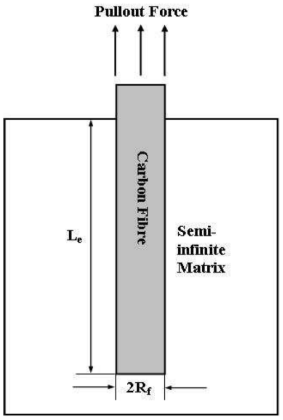

Figure 2: A Schematic Diagram of the Fibre Pull-Out Model
Reproduced with kind permission from Jia, Yan and Liu (2011)

In conjunction with Figure 2, the geometry of the model included a concentric cylinder, acting as the matrix surrounding the fibre; the carbon fibre itself, embedded at length (L_e) with a diameter of twice the fibre radius (R_f) situated in the centre of the matrix.

Abaqus Finite Element Analysis Software was used to perform the pull-out simulation in the original study. However, for this piece of research Ansys Engineering Simulation and 3D Design Software was used instead. A 2D-Axisymmetric model was constructed as opposed to that of a 3D model due to the symmetry in nature. An advantage of using this type of model was that it significantly reduced the overall elapsed analysis time.

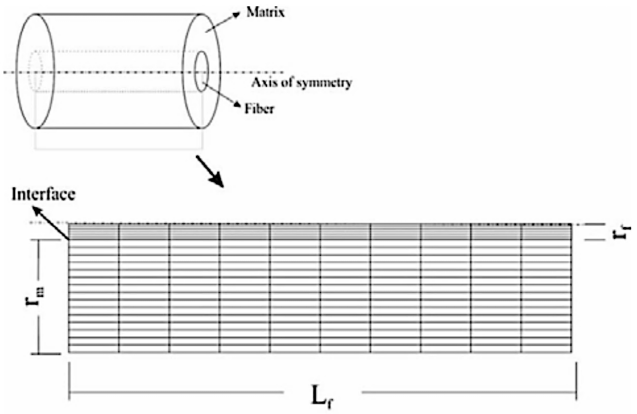

Figure 3: Axisymmetric Concentric-Cylinder Model and Mesh
Reproduced with kind permission from Friedrich and Wang (2019)

Geometry

A 2D-Axisymmetric model of the composite was constructed in Ansys 19.2. The fibre radius (R_f) used in the geometric model below was 3.5μm and the depth in which the fibre was embedded (L_e) in the epoxy matrix was 100μm.

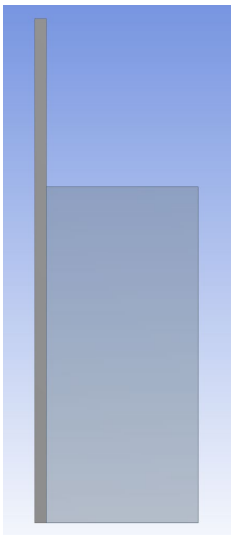

Figure 4: Geometry of 2D-Axisymmetric Model

Material Properties

Both the carbon fibre and epoxy matrix are linear elastic and isotropic in nature. The key mechanical properties for both materials are shown below.

Table 1: Mechanical Properties of Carbon Fibre and Epoxy
Reproduced with kind permission from Jia, Yan and Liu (2011)

Mechanical Properties	Carbon Fibre	Epoxy Matrix
Young's Modulus (GPa)	238	3.4
Poisson's Ratio	0.28	0.2

Interface

The implementation of a cohesive zone functions primarily to model the progressive debonding failure at the interface between the two materials in contact. CZM permits three separation modes, namely mode I (debonding for normal separation), mode II (debonding for tangential separation) and mixed mode (debonding for normal and tangential separation). However, as this model in particular deals with the replication of a pull-out simulation, debonding for tangential separation was the chosen separation mode.

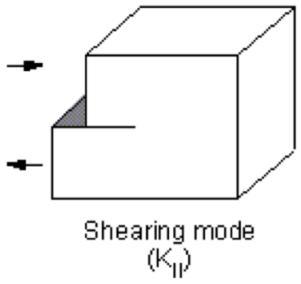

Figure 5: Mode II Debonding

Under mode II conditions, the behaviour of materials at the interface are governed by both tangential stresses and tangential sliding.

Cohesive Zone – Separation-Distance Based Debonding

The table below provides properties for the Interfacial Element. These values were obtained from the existing study (Jia, Yan and Liu, 2011).

Table 1: Interfacial Element Properties for Mode II Debonding
Reproduced with kind permission from Jia, Yan and Liu (2011)

Interfacial Element Properties	Separation-Distance Based Debonding
Debonding Interface Mode	Mode II
Maximum Equivalent Tangential Contact Stress (MPa)	45
Tangential Slip at the Completion of Debonding (μm)	25
Artificial Damping Coefficient (s)	0.000001

Contact Region

The contact region (red line) was detected between the edges connecting the carbon fibre (left) and the epoxy matrix (right).

Figure 6: Magnified Contact Region

The contact body in this model was the epoxy matrix. The edge in contact with the carbon fibre consisted of CONTA172 elements that were used to represent both contact and sliding between 2D target surfaces.

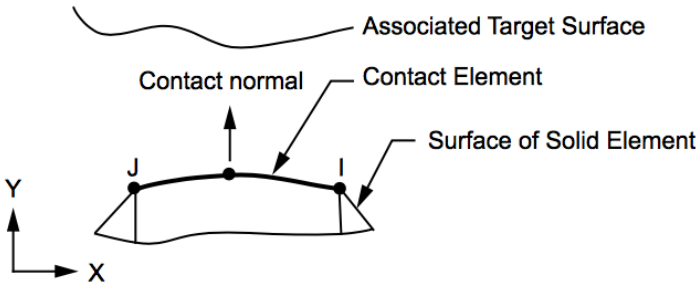

Figure 1: CONTA172 Geometry

The target body in this model was the carbon fibre. The edge in contact with the epoxy matrix consisted of TARGE169 Elements that were used to represent the 2D target surfaces for the associated contact element (CONTA172).

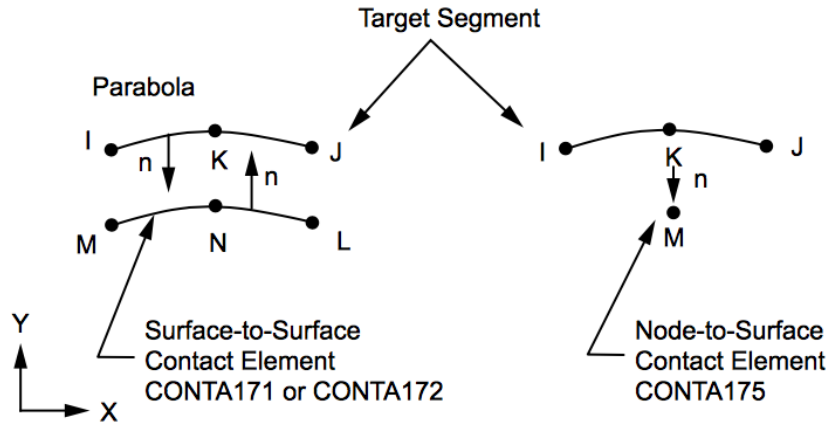

Figure 8: TARGE169 Geometry

A bonded contact and pure penalty formulation was applied to the model. The pure penalty method was highly dependent on the contact stiffness. If the contact stiffness was too large it would result in convergence difficulties, however the model had the ability to oscillate. The Artificial Damping Coefficient (η) was used to stabilise the numerical solution but would only be effective if it were smaller than the size of the minimum time step. In this case, η was 1 x 10^{-6} s whilst the minimum time step was 1 x 10^{-5} s.

Meshing

A fine mesh of varying size was used on this model. The element size for the epoxy matrix was set at a default of 6.36μm, whilst for the carbon fibre it was set as 1μm. An edge sizing of 1μm was applied to the 2 edges located at the interfacial zone. The small element size at the interface was vital for ensuring the accuracy of the numerical results. A quadrilateral dominant method was used across both material surfaces with a face mesh type of quad/tri.

PLANE183 elements were adapted to this 2D-Axisymmetric model due to the irregularity in meshing. Quadrilateral elements consisted of 8-nodes whilst triangular elements consisted of 6-nodes, each of which were constrained to having two degrees of freedom.

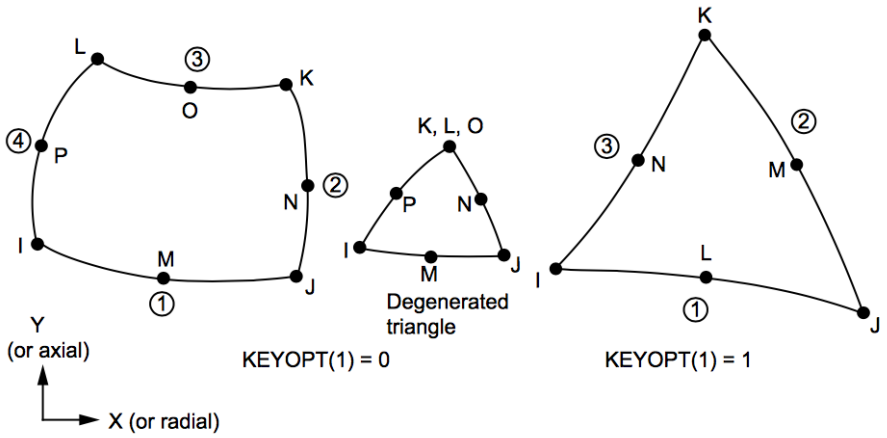

Figure 9: PLANE183 Geometry

The figures below show the comparison between meshing for the model in both Abaqus and Ansys Software.

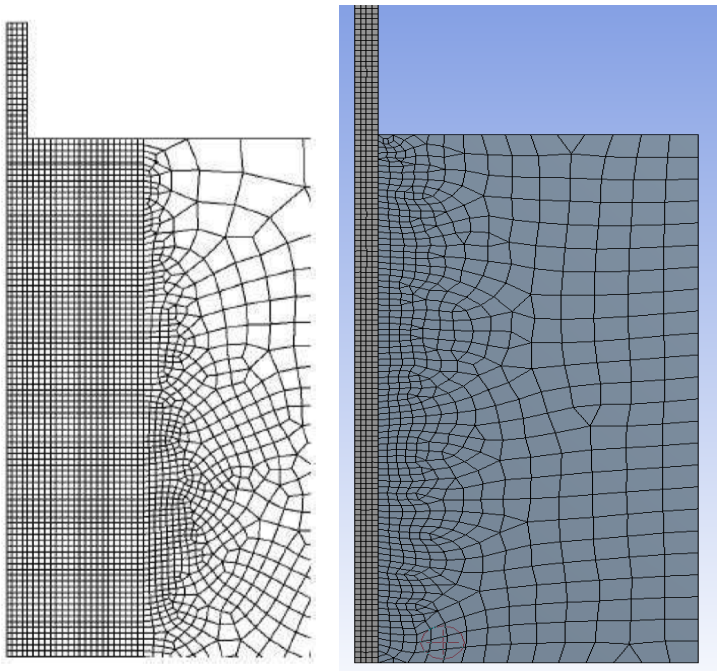

Figure 10: Meshing of 2D-Axisymmetric FE Model (Left) Abaqus (Right) Ansys
Reproduced with kind permission from Jia, Yan and Liu (2011)

Boundary Conditions

The top edge of the epoxy matrix was constrained in both the radial and axial directions by setting both the x and y components as 0μm. On the carbon fibre, a displacement was applied to the top edge in the axial direction and constrained in the radial direction. The x-component was set as 0μm, whilst the y-component was set as 50μm.

Experimental Pull-Out Test

Due to the lack of research regarding the interfacial debonding behaviour between carbon fibre textile and concrete meant that experimental testing was the only method of obtaining data that could be used in the process of numerical modelling.

Pull-Out Trial with Small Cylinder

All information regarding the pull-out trial was obtained from a study conducted by a Civil Engineering Ph.D Student from Plymouth University (Ji, 2019).

Material Properties

The carbon fibre tow used in the experiment consisted of 24 thousand individual fibres; each of which was adhered together using polymer. The key properties for the tow are shown in the table below.

Table 2: Properties of 24K Carbon Fibre Tow
Reproduced with kind permission from Ji (2019)

24K Carbon Fibre Tow			
Mechanical Properties		**Geometric Properties**	
Theoretical Maximum Tensile Force (kN)	1.489	Theoretical Cross-Sectional Area (mm^2)	0.876

The tables below show a breakdown of the ratios and quantities of the different components that make up the matrix surrounding the carbon fibre tow.

Table 3: Matrix Mix Ratio
Reproduced with kind permission from Ji (2019)

Ratio of Binding Materials (%)				**w/b**	**Concrete Mix Ratio (kg/m^3)**			
Cement	PFA	GGBS	Silica Fume		Binder	Sea Sand	Sea Water	Water Reducer
55	20	20	5	0.3	685	1370	205.5	6.85

Materials Dosage (kg): (Mortar **2267.35** kg/m^3; Actual Value = Design Value*1.3 = 6.040 kg)

Table 4: Matrix Material Dosage
Reproduced with kind permission from Ji (2019)

Cement	***PFA***	***GGBS***	***Silica Fume***	***Sea Sand***	***Sea Water***	***Water Reducer***
1.004	0.365	0.365	0.091	3.650	0.547	0.018

Preparation and Set-Up of Materials

The carbon fibre tow used in the experiment was 200mm long. A layer of epoxy resin was applied to 110mm of the tow then treated with sand.

Figure 11: Sand Treated Carbon Fibre Tow
Reproduced with kind permission from Ji (2019)

The concrete cylinder used for testing had a height of 50mm and diameter of 22.2mm. Prior to casting the concrete into the cylindrical mould, the carbon fibre tow was positioned at the desired length of embedment. In this case, the bond length between the tow and matrix was equivalent to the height of the cylinder. A stainless-steel tube with a length of 100mm and diameter of 5mm attached to a section of the carbon fibre tow that had not been treated with sand. The actual bond length between the tube and the tow was 90mm. The specimen was then connected to the testing rig in order to begin the pull-out procedure.

Figure 12: Carbon Fibre Tow Specimen Embedded in Concrete Cylindrical Matrix (Left)
Pull-Out Test Set-Up (Right)
Reproduced with kind permission from Ji (2019)

Finite Element Modelling of the Modified CZM

The second finite element model was modified in order to replicate the simulation of a single carbon fibre tow from a concrete matrix. Data provided for the FE model came from an experiment conducted in a laboratory at Plymouth University.

Geometry

As with the initial model, the modified CZM remained as a 2D-Axisymmetric model. The fibre radius (R_f) of the carbon tow used in the geometric model was 0.5mm and the depth in which the fibre was embedded in the concrete matrix was 50mm.

Material Properties

Both the carbon fibre tow and concrete matrix are linear elastic and isotropic in nature (as with the previous FE model). The key mechanical properties for both materials are shown below.

Table 5: Mechanical Properties of Carbon Fibre Tow and Concrete

Mechanical Properties	Carbon Fibre Tow	Concrete Matrix
Young's Modulus (GPa)	150	30
Poisson's Ratio	0.28	0.2
Tensile Yield Strength (MPa)	1030.039	-
Tensile Ultimate Strength (MPa)	1489	-

Interface

Cohesive Zone – Separation-Distance Based Debonding

The table below provides properties for the interfacial element. These values were obtained by means of trial and error in order to produce a maximum pull-out force (F_{max}) that matched up close enough with that of the experiment.

Table 6: Interfacial Element Properties for Mode II Debonding

Interfacial Element Properties	Separation-Distance Based Debonding
Debonding Interface Mode	Mode II
Maximum Equivalent Tangential Contact Stress (MPa)	6.475
Tangential Slip at the Completion of Debonding (mm)	0.775
Artificial Damping Coefficient (s)	0.000001

Contact Region

The contact region for the model was detected between the edges connecting the carbon fibre tow and concrete matrix (as with the previous FE model). The contact body in this model was the concrete matrix, whilst the target body was the carbon fibre tow. CONTA172 elements were located along the edge of the concrete matrix in contact with the carbon fibre tow, whilst TARGE169 elements were located along the edge of the carbon fibre tow in contact with the concrete matrix.

A bonded contact and pure penalty formulation had also been applied to the model. Both the artificial damping coefficient **(η)** and minimum time step remained the same as with the previous model.

Meshing

The method of meshing for the modified CZM remained the same as that of the initial model. However, both the element size for the carbon fibre tow and the edge sizing was set as 0.1mm.

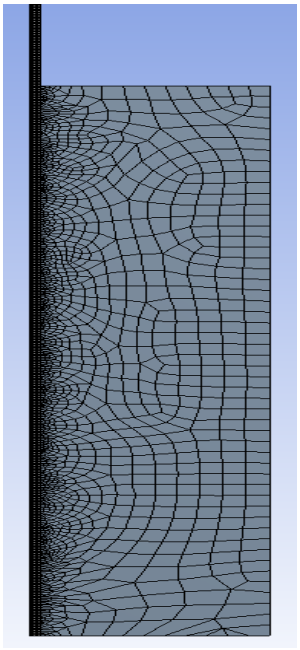

Figure 13: Meshing of 2D-Axisymmetric Finite Element Model

PLANE183 elements were also adapted to this 2D-Axisymmetric model. Figure 14 shows a magnification on the meshing between the surfaces of the carbon fibre tow and concrete matrix.

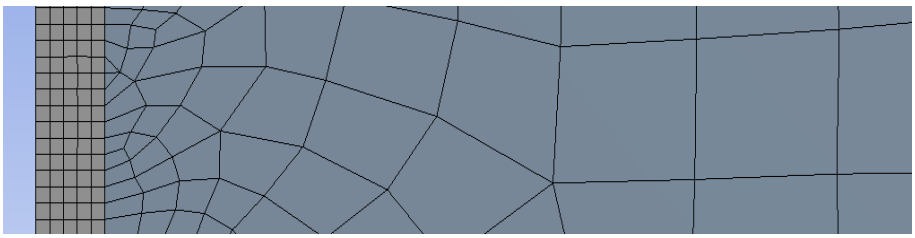

Figure 14: Magnification of Meshing on 2D-Axisymmetric Model

Boundary Conditions

The top edge of the concrete matrix was constrained in both the radial and axial directions by setting both the x and y components as 0mm. On the carbon fibre, a displacement was applied to the top edge in the axial direction and constrained in the radial direction. The x-component was set as 0mm, whilst the y-component was set as 2mm.

Discussion

Results of the Initial CZM

As previously mentioned, the purpose of the initial CZM was to provide a basic framework for the numerical model to be used in the current study. Figure 15 illustrates the interfacial debonding behaviour between carbon fibre and an epoxy matrix by means of a force – pull-out displacement curve, produced from the existing study (Jia, Yan and Liu, 2011) using Abaqus. The graph clearly shows a good correlation between the experimental results that the study used in order to create their numerical model and the results obtained through the finite element simulation. The maximum pull-out force (debonding force) produced from the FE simulation was 0.096N against a value of 0.1N from the experiment.

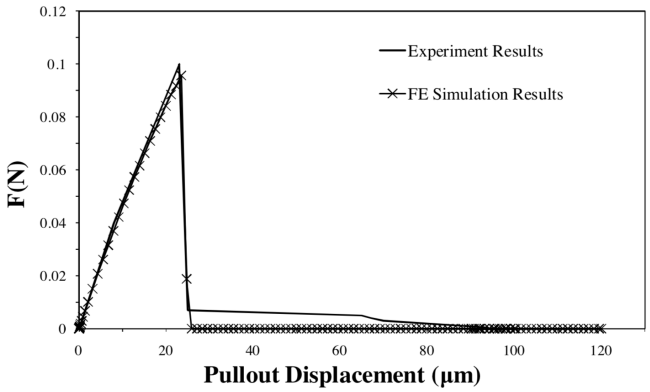

Figure 15: Force - Displacement Curves for Carbon Fibre Pull-Out Test Produced using Abaqus
Reproduced with kind permission from Jia, Yan and Liu (2011)

Figure 16 shows the force – pull-out displacement curve produced from Ansys. The debonding produced from the FE simulation was 0.098N. This result matches up very well with the values from the previous graph, suggesting that the numerical model has been correctly implemented and is producing results that are consistent with its intended purpose.

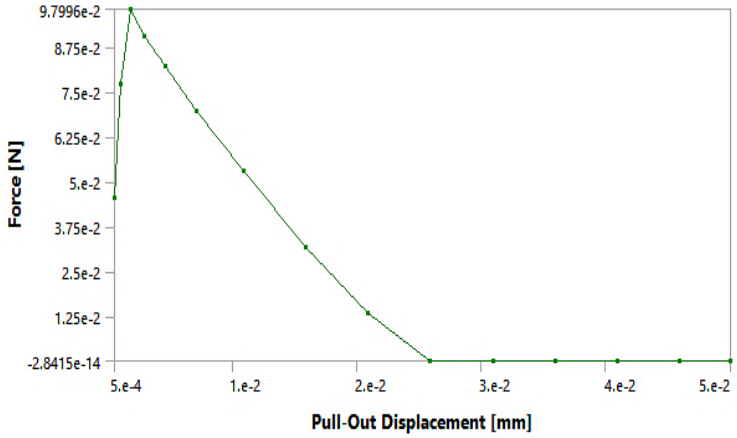

Figure 16: Force - Displacement Curve for Carbon Fibre Pull-Out Test Produced using Ansys

F_{max} in both graphs correspond to an initiate crack separation displacement (δ_d). In Figure 15, δ_d is equivalent to 20μm whilst in Figure 16, δ_d corresponds to 1.75μm. A possible reason for this difference might be due the Artificial Damping Coefficient (η) defined for the Interfacial Element. This value can affect the overall solution as soon as the initial crack starts to propagate along the interface. This would therefore suggest that the η (1 x 10^{-6} s) used for the model created in Ansys might be more accurate compared to the one used in Abaqus, as δ_d was detected much sooner.

Another possible explanation might be due to the analysis settings; specifically, the step controls. In Ansys, steps are defined by time (s). The initial time step was 0.01s; the minimum time step was 0.00001s and the maximum time step was 0.1s. It is possible that the time step used in the Abaqus model might be larger, which could account for why crack initiation failed in being detected sooner. It is also possible that a completely different method of analysis was used.

In relation to the Cohesive Zone Law, the steepness of the slope representing the Stiffness is affected by the corresponding values for δ_d; meaning that a steeper slope is caused by a smaller δ_d. As a result, differences in either the artificial damping coefficient (η) or analysis settings could have contributed to the variation in δ_d.
The point in which the force returns to 0N represents the complete separation displacement (δ_s). This value is equivalent to 25μm in both graphs. δ_s suggests that the interface between the carbon fibre and epoxy has fully disintegrated and can therefore be completely pulled out from the matrix.

Results of the Experimental Pull-Out Test
The second finite element model was based on the results obtained from an experimental pull-out test (Ji, 2019). Figure 17 shows the force – pull-out displacement curve.

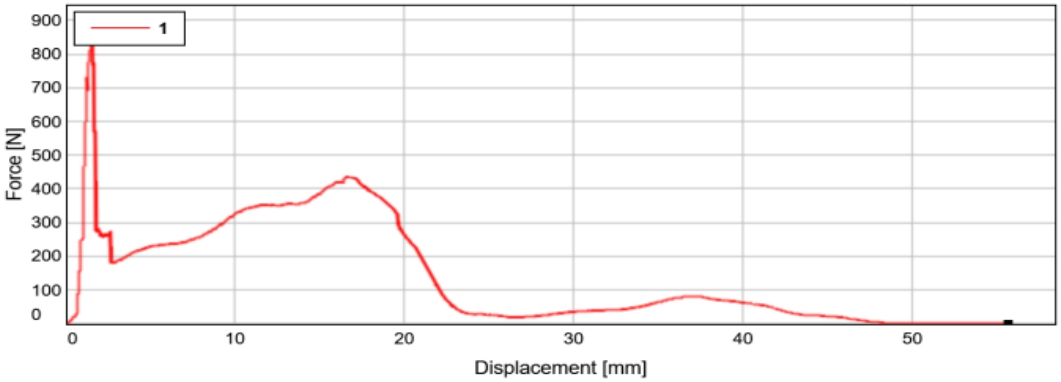

Figure 17: Force - Displacement Curve Based on Pull-Out Test Data
Reproduced with kind permission from Ji (2019)

The force – pull-out displacement curve is a global representation of the bond stress – slip relationship between the carbon fibre tow and concrete matrix. It demonstrates how the pull-out load gradually increases, but then comes to a halt as it reaches its F_{max}, which in this case is 902.1N. Up until this point, the interfacial bond was governed purely by the adhesion and frictional forces occurring between the tow and matrix. From this point onwards, the process of debonding progressively weakens the

interface due to the failure of adhesion. The remaining part of the graph illustrates the effect the sand treatment had on the pull-out behaviour of the carbon fibre tow from the concrete matrix.

Table 8 provides the basic mechanical parameters obtained from the experiment.

Table 7: Mechanical Parameters obtained from Pull-Out Experiment

Peak Load (kN)	*Displacement at Peak Value (mm)*	*Total Displacement (mm)*	*Tensile Strength (MPa)*	*Bond Strength (MPa)*
0.9021	1.6318	55.68	1030.039	5.439

The bond strength was calculated using the equation,

$$\tau = F_{max}/\pi\phi L_e$$

Results of the Modified CZM

Figure 18 shows the force – pull-out displacement curve produced from Ansys. Evidently the maximum tensile force of 0.9021kN from the experiment correlates very well with the maximum tensile force of 0.9082kN from the numerical model created in Ansys.

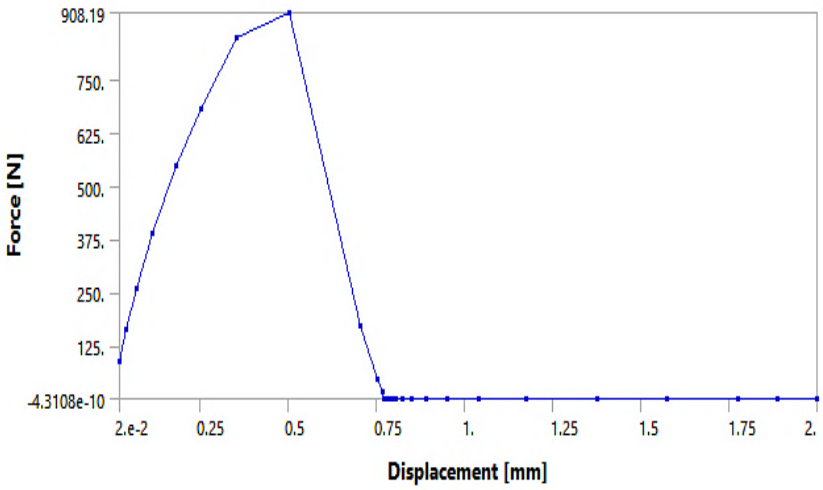

Figure 18: Force - Displacement Curve Produced using Ansys

The experimental peak load was used as a rough guide to calibrate both the maximum equivalent tangential contact stress and the tangential slip at the completion of debonding. Through numerous trials and a series of adjustments, the carbon fibre tow – concrete matrix interface was found to have a maximum shear stress (τ_{max}) of 6.475MPa at a complete separation displacement (δ_s) of 0.775mm. It is important to be cautious of the fact that the calibrated values for the τ_{max} and δ_s include the effect

of additional frictional resistance from the sand-treated surface of the carbon fibre tow. As mentioned in the study conducted by Baena et al. (2009), sand-coated carbon fibre is expected to produce a higher bond strength in comparison to textured carbon fibre. Therefore, if the experiment was repeated using an untreated carbon fibre tow there is a high likelihood that recalibration of the experimental peak load would result in a smaller τ_{max}. Figure 19 is a representation of the local bond stress – slip occurring at the interface.

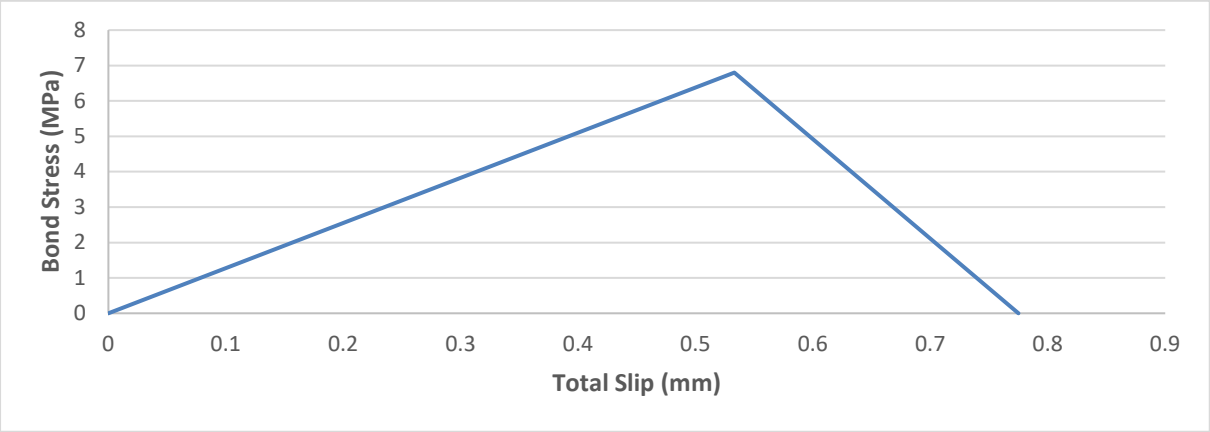

Figure 19: Interfacial Bond - Stress Slip

Table 9 provides a comparison between the global and local debonding of the carbon fibre tow and concrete matrix. The bond strength calculated from the experiment was approximately 1.036MPa smaller compared to the τ_{max} obtained from the numerical model. As the values are not significantly different, this would suggest that the simplified equation $\tau = P/\pi\phi L$ gives a reasonable approximation of the maximum shear stress.

Table 8: Comparison between Global and Local Debonding Parameters

Global Debonding (Experimental Testing)		**Local Debonding (Numerical Model)**	
Peak Load (kN)	0.9021	*Peak Load (kN)*	0.9082
Bond Strength (MPa)	5.439	*Maximum Shear Stress (τ_{max}) (MPa)*	6.475
Displacement at Peak Value (mm)	1.6318	*Initiate Crack Separation Displacement (δ_d) (mm)*	0.50313
Total Displacement (mm)	55.68	*Complete Separation Displacement (δ_s) (mm)*	0.775

Parametrical Study

The maximum pull-out force, otherwise known as the 'Debonding Force' is the most vital parameter to be obtained from a pull-out experiment, as it is required in order to determine the interfacial bond strength. F_{max} is a function of numerous parameters,

$$F_{\max}=f\left(\tau_{\max},\delta_d,\delta_s,R_f,L_e,E_f,E_m,\nu_f,\nu_m,\mu\right)$$

Finite Element (FE) simulations are particularly useful as they numerically investigate the influence that each parameter has on the debonding force (F_{max}). This section will focus on understanding the effect that the geometric properties of the carbon fibre tow have on the F_{max}. These parameters will be investigated using the numerical model produced for this current study.

Effect of Fibre Radius (R_f)

The effect of the R_f is shown in Figures 20 and 21. The relationship shows how increasing or decreasing the fibre radius both result in a linear increase of the F_{max} with respect to the pull-out displacement. The pull-out forces corresponding to the 1mm R_f appear to be significantly higher than the forces corresponding to the 0.25mm R_f.

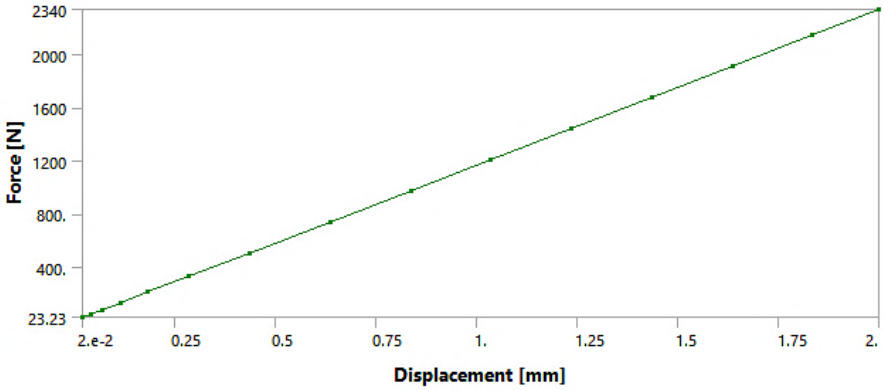

Figure 20: Force - Displacement Curve for 0.25mm Fibre Radius

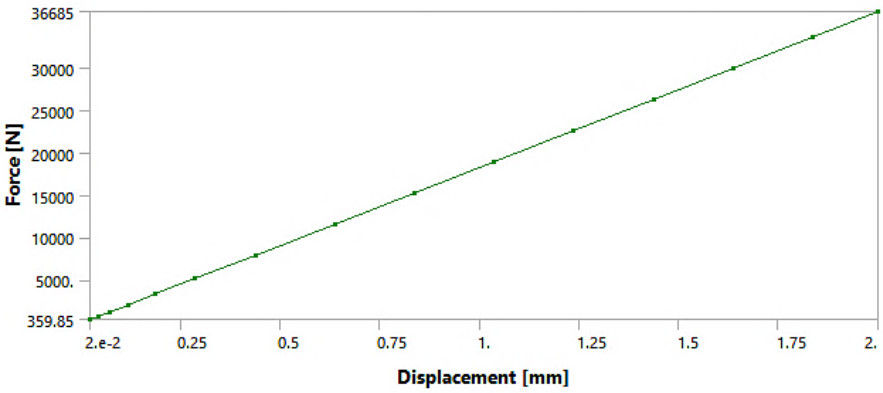

Figure 21: Force - Displacement Curve for 1mm Fibre Radius

Effect of Embedded Length (L_e)

The effect of the L_e is shown in Figures 22 and 23. Similar to the effect of the R_f, the relationship also shows how changing the Embedment Length results in a linear increase of F_{max} with respect to the pull-out displacement. The pull-out forces corresponding to the 60mm L_e appear to be significantly higher than the forces corresponding to the 40 mm L_e.

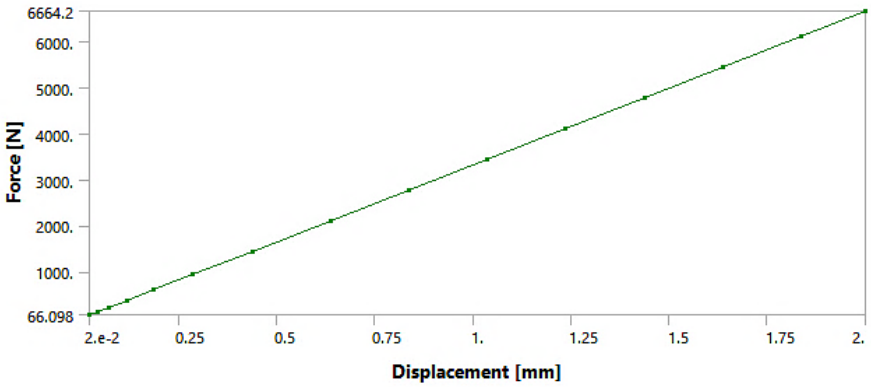

Figure 22: Force – Displacement Curve for 40mm Embedment Depth

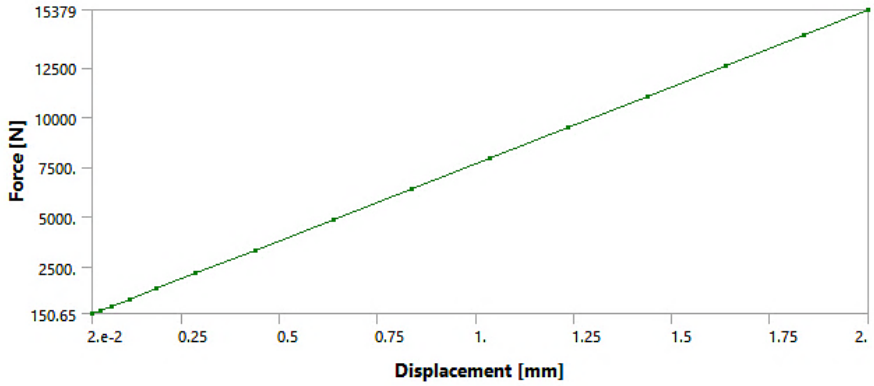

Figure 23: Force – Displacement Curve for 60mm Embedment Depth

Limitations

A major limitation of this study was due to the lack of experimental data available regarding the pull-out of a carbon fibre tow from a concrete matrix. The numerical model created in this study calibrated vital interfacial parameters based on a single set of results. This could potentially prove to be quite inaccurate, resulting in unreliable findings. Aside from this, no other numerical models regarding the interfacial behaviour of carbon fibre – concrete were found that could be used for comparison purposes. This therefore made it difficult to assume whether or not τ_{max} and δ_s was calibrated to a reasonable tolerance.

Recommendations

A key recommendation for this study is to collect multiple experimental results from carbon fibre – concrete pull-out tests in order to improve not only the accuracy of the calibrated τ_{max} and δ_s, but also the overall reliability and validity of the findings. It is also recommended that the pull-out tests conducted do not use carbon fibre specimens treated with a sand coating. This is to ensure that the calibrated τ_{max} and δ_s are representing true interfacial behaviour.

Conclusions

In conclusion, it is clear to see that the numerical model generated using Ansys was successfully able to replicate not only the conditions of the experimental pull-out simulation but also produced a maximum pull-out force that correlated very well with the experimental results:

$$F_{max}\text{ (Experimental)} = 0.9021\text{kN}$$
$$F_{max}\text{ (Numerical Model)} = 0.9082\text{kN}$$

Evidently the CZM conforms to the Cohesive Zone Law in that an increase in pull-out force equates to an increase in bond strength up until the point in which F_{max} is reached. F_{max} represents the point in which the debonding begins due to the formation of cracks. These cracks continually propagate along the interface until there is physically no contact between the carbon fibre and concrete. At this point, adhesion has completely failed.

The debonding force (F_{max}) produced from the experiment was the key parameter required for calibrating the values for both the maximum shear stress (τ_{max}) and complete separation displacement (δ_s).

$$\tau_{max} = 6.475\text{MPa}$$
$$\delta_s = 0.775\text{mm}$$

Although these interfacial values match up well with the experimental F_{max} value, they are in no way representative of the true interfacial behaviour. More experiments would need to be carried out in order to increase the accuracy, reliability and overall validity of the findings.

Acknowledgements

This project would not have been possible without the continuous help and support from various individuals. Firstly, I would like to express my deepest gratitude for my dissertation supervisor Dr. Shanshan Cheng, for taking the time to guide and assist the project, but more importantly for being there to offer her advice throughout the many challenging stages. I would also like to thank my family and friends; namely Bryony Brimble, Hassan Chaudhry and Jayaram Surendirarasa for being such an incredible support system throughout this difficult journey to completing my dissertation. Finally, I would like to thank the almighty God for being my strength and inspiring me to never give up.

References

Baena, M., Torres, L., Turon, A. and Barris, C. (2009). Experimental study of bond behaviour between concrete and FRP bars using a pull-out test. *Composites Part B: Engineering*, 40(8), pp.784-797.

Barenblatt, G. (1959). The formation of equilibrium cracks during brittle fracture. General ideas and hypotheses. Axially-symmetric cracks. *Journal of Applied Mathematics and Mechanics*, 23(3), pp.434-444.

De Lorenzis, L. and Zavarise, G. (2009). Cohesive zone modeling of interfacial stresses in plated beams. *International Journal of Solids and Structures*, 46(24), pp.4181-4191.

Dugdale, D. (1960). Yielding of steel sheets containing slits. *Journal of the Mechanics and Physics of Solids*, 8(2), pp.100-104.

Fitzcr, E. (1990). Carbon Fibers Filaments and Composites. Herausgeg. vonJ. L. Figueiredo,C. A. Bernardo,R. T. K. BakerandK. J. Hüttinger. Kluwer Academic Publishers Group, Dordrecht 1989. XII, 381 S., zahlr. Abb. u. Tab., geb., US $ 148,-. *Chemie Ingenieur Technik*, 63(7), pp.3-41.

Friedrich, L. and Wang, C. (2016). Continuous Modeling Technique of Fiber Pullout from a Cement Matrix with Different Interface Mechanical Properties Using Finite Element Program. *Latin American Journal of Solids and Structures*, 13(10), pp.1937-1953.

Guide for the Design and Construction of Structural Concrete Reinforced with FRP Bars. (2006). [ebook] Available at: http://www.radyab.co/content/media/article/13.pdf [Accessed 5 Dec. 2018].

Hsueh, C. (1990). Interfacial debonding and fiber pull-out stresses of fiber-reinforced composites. *Materials Science and Engineering: A*, 123(1), pp.1-11.

Ji, Jie. (2019) *Durability Research on Carbon Fibre Textile Reinforced Mortar*. Internal research report (University of Plymouth). Unpublished

Jia, Y., Yan, W. and Liu, H. (2011). *Numetrical Study on Carbon Fibre Pullout Using a Cohesive Zone Model*. [ebook] Available at: https://www.iccm-central.org/Proceedings/ICCM18proceedings/data/2.%20Oral%20Presentation/Aug24%28Wednesday%29/W24%20Delamination%20and%20Interlaminar%20Reinforcement/W24-2-AF0936.pdf [Accessed 1 Nov. 2018].

Lin, X. and Zhang, Y. (2014). Evaluation of bond stress-slip models for FRP reinforcing bars in concrete. *Composite Structures*, 107, pp.131-141.

Liu, H., Zhou, L. and Mai, Y. (1995). Effect of Interface Roughness on Fiber Push-Out Stress. *Journal of the American Ceramic Society*, 78(3), pp.560-566.

Sólyom, S. and Balázs, G. (2015). BOND STRENGTH OF FRP REBARS. [ebook] Available at:

https://www.researchgate.net/publication/308688068_Bond_strength_of_FRP_rebars [Accessed 28 Nov. 2018].

Sólyom, S., Balázs, G. and Borosnyói, A. (2015). MATERIAL CHARACTERISTICS AND BOND TESTS FOR FRP REBARS. [online] Available at: http://www.fib.bme.hu/folyoirat/cs/cs2015.pdf [Accessed 28 Nov. 2018].

Sonnenschein, R., Gajdosova, K. and Holly, I. (2016). FRP Composites and their Using in the Construction of Bridges. *Procedia Engineering*, 161, pp.477-482.

Täljsten, B. (1996). Strengthening of concrete prisms using the plate-bonding technique. *International Journal of Fracture*, 82(3), pp.253-266.

Teng, J., Yuan, H. and Chen, J. (2006). FRP-to-concrete interfaces between two adjacent cracks: Theoretical model for debonding failure. *International Journal of Solids and Structures*, 43(18-19), pp.5750-5778.

Tsai, J., Patra, A. and Wetherhold, R. (2005). Finite element simulation of shaped ductile fiber pullout using a mixed cohesive zone/friction interface model. *Composites Part A: Applied Science and Manufacturing*, 36(6), pp.827-838.

Zhang, X. (1999). On steady-state fibre pull-outI The stress field. *Composites Science and Technology*, 59(15), pp.2179-2189.